Proceedings of the Edinburgh Mathematical Society (2016) **59**, 287–300
DOI:10.1017/S0013091515000139

STOCHASTIC MODELS FOR CHLADNI FIGURES

JAIME ARANGO[1] AND CARLOS REYES[2]

[1]*Departamento de Matemáticas, Universidad del Valle, Calle 13, 100-00, Cali, Colombia* (jaime.arango@correounivalle.edu.co)
[2]*Posgrado de Matemáticas, Universidad del Valle, Calle 13, 100-00, Cali, Colombia*

(Received 22 July 2013)

Abstract Chladni figures are formed when particles scattered across a plate move due to an external harmonic force resonating with one of the natural frequencies of the plate. Chladni figures are precisely the nodal set of the vibrational mode corresponding to the frequency resonating with the external force. We propose a plausible model for the movement of the particles that explains the formation of Chladni figures in terms of the stochastic stability of the equilibrium solutions of stochastic differential equations.

Keywords: Chladni figures; clamped plates; free plates; stability; stochastic differential equations; wave equation

2010 *Mathematics subject classification:* Primary 60H30
Secondary 74H50; 60H10; 74K20

1. Introduction

In the late eighteenth century Chladni observed that sand randomly scattered across a plate assumed beautiful patterns as the border of the plate was excited with a particular pitch using the bow of a violin. Chladni's observation can be roughly explained as a resonant phenomenon when the frequency of the exciting force coincides with one of the natural frequencies of the plate. Essentially, the patterns, which are known as Chladni figures, are the nodal set of the vibrational mode whose frequency resonates with the external force. We recall that the nodal set N_ϕ of the vibrational mode ϕ is defined by

$$N_\phi = \{x \in \bar{U} \colon \phi(x) = 0\}.$$

In this paper we propose a stochastic model that takes into account the wiggly motion of the particles when the external force resonates with one of the natural frequencies of the plate, say that frequency corresponding to the vibrational mode ϕ. As the experimentation shows, the motion of the particles resembles that of Brownian motion, yet the particles jump further and the jumps become more dispersed near the local extrema of ϕ, while in the neighbourhood of the nodal lines of ϕ, the particles settle down. Further, one expects particles to have, on average, a horizontal velocity component opposite to the

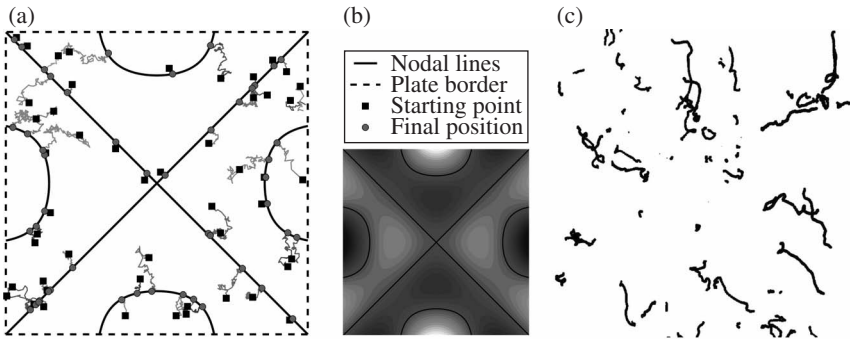

Figure 1. (a) Trajectories of the SDE (1.1) (for $\alpha = 2$, $\beta = 1$) converging to the nodal lines of the mode ϕ, whose contours are pictured in (b). Experimental trajectories of particles were captured for the same mode ϕ and are shown in (c).

gradient of the vibrating mode after bouncing against the bending plate. Accordingly, it seems reasonable that the random dynamics governing the particles' motion has a drift direction contrary to $\nabla\phi$ and a diffusion component somehow proportional to ϕ.

Laboratory experiments with iron plates, numerical experimentation with stochastic differential equations (SDEs) and some elementary physical considerations suggest that the random dynamics of the moving particles obey an SDE similar to

$$\mathrm{d}X_t = -\alpha\phi(X_t)\nabla\phi(X_t)\,\mathrm{d}t + \beta\phi(X)\,\mathrm{d}W_t, \quad X_0 = x, \tag{1.1}$$

where W_t is a standard two-dimensional Brownian motion, ϕ is a vibrational mode of the plate defined on a planar region U (the plate at rest), and $\alpha \geqslant 0$ and $\beta \in \mathbb{R}$ are constants. According to this model, the particles move in one among many possible trajectories of the SDE starting at some point $x \in U$. The main result of this paper establishes that non-critical points belonging to the nodal set of ϕ, i.e. points in N_ϕ at which $\nabla\phi$ does not vanish, are stochastically stable equilibria of a class of SDEs of which (1.1) is a particular case. Setting $\alpha = 0$ in (1.1), we improve the stability result to cover all but isolated points of the nodal set N_ϕ.

To summarize our investigation, we refer to Figure 1, illustrating in the centre the level sets of a vibrational mode ϕ of a free square plate. In part (a) we see several trajectories of SDE (1.1) converging to the nodal lines of ϕ. The reader may compare these trajectories with those obtained experimentally (Figure 1(c)) and captured using the library for image processing, OpenCV [**2**].

Figure 2(b) shows the final positions of the trajectories starting at an initial grid of 360 random points uniformly distributed on the unit square (part (a)). Our goal is to show that the outcomes pictured in Figures 1 and 2 are typical for all vibrational modes of plates under free or clamped boundary conditions.

In this paper we model Chladni's experiment as a stochastic process defined by the solutions of a more general SDE,

$$\mathrm{d}X_t = \mu_\phi(X_t)\nabla\phi(X_t)\,\mathrm{d}t + \sigma_\phi(X_t)\,\mathrm{d}W_t, \quad X_0 = x, \tag{1.2}$$

where μ_ϕ and σ_ϕ fulfil the following conditions.

https://doi.org/10.1017/S0013091515000139 Published online by Cambridge University Press

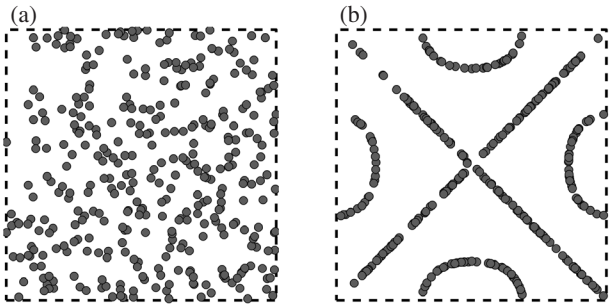

Figure 2. (a) An initial grid of 360 random points uniformly distributed on a square of side 1. (b) Final positions of the trajectories of the SDE (1.1) (for $\alpha = 2$, $\beta = 1$) after time $t = 10$.

Assumption 1.1. μ_ϕ and σ_ϕ are 2×2 continuous matrix-valued functions such that (1.2) has a unique solution defined for all $t \geqslant 0$ and

(1) $\mu_\phi(x) = 0$ and $\sigma_\phi(x) = 0$ for all $x \in N_\phi$;

(2) the drift matrix $\mu_\phi(x)$ satisfies $\mu_\phi(x) = f(\phi(x))\nu_\phi(x)$, where $\nu_\phi(x)$ is positive definite for all $x \in N_\phi$ with $\nabla\phi(x) \neq 0$ and f is a scalar odd Lipschitz function that either identically vanishes or is negative in some interval $(0, \varepsilon)$, $\varepsilon > 0$;

(3) there exists a uniformly positive definite matrix A, such that its coefficients are Hölder continuous and

$$\sigma(x)\sigma^{\mathrm{Tr}}(x) = (\sigma_{11}^2(x) + \sigma_{22}^2(x))A(x)$$

in a neighbourhood of $\bar{U}$, where $\sigma(x) \equiv \sigma_\phi(x)$.

Despite its apparent simplicity, Chladni's experiment hides quite complicated physical processes beneath the movement of the particles. It was known by Chladni himself that finely granulated particles, ground table salt for example, collect not near the nodal lines, as normal sand or salt would collect, but close to the local extrema of ϕ (the antinodes of the plate motion). The full explanation of this was given by Faraday [**5**], but not until 1830.

In § 2 we review the basic facts on the transverse vibration of a plate, define the vibrational modes of a plate and go over some well-known cases in which the modes of vibration ϕ can be computed explicitly (sort of). In § 3 we give a justification for the stochastic model and prove the stability results (see Theorems 3.2 and 3.4). One important assumption we made for these results is that the nodal set has no isolated points.

2. The transverse vibration of a plate

The goal of this section is to define the vibrational modes of a plate as the solutions of an eigenvalue problem. We refer the reader to [**7**] and references therein for a recent account on Chladni figures and the mathematical model for vibrations of plates.

https://doi.org/10.1017/S0013091515000139 Published online by Cambridge University Press

Let us consider a plate of constant thickness h made up of a uniform material with density ρ, Poisson ratio ν and Young's modulus of elasticity E, vibrating due to an external force $F(t,x,y)$. Let us write $u(t,x,y)$ to denote the vertical position of the plate at a point (x,y) at time t. According to the classical theory of plate vibration, we have

$$D\Delta^2 u + \rho h \frac{\partial^2 u}{\partial t^2} = F(t,x,y), \quad t \geqslant 0,\ (x,y) \in U, \tag{2.1}$$

where

$$D = \frac{Eh^3}{12(1-\nu^2)}, \qquad \Delta^2 u = \frac{\partial^4 u}{\partial x^4} + 2\frac{\partial^4 u}{\partial x^2 y^2} + \frac{\partial^4 u}{\partial y^4}$$

and U is a planar bounded region that we identify with the plate at rest. The constant D is known as the flexural rigidity of the plate and Δ^2 is called the biharmonic operator. Notice that $\Delta^2 u = \Delta(\Delta u)$, where Δ is the Laplace operator.

Regarding the boundary conditions, we suppose that the plate is either free or clamped at the border ∂U. The conditions (free or clamped) that a solution u satisfies at the boundary are denoted by

$$B(u) = 0 \quad \text{on } \partial U.$$

Later on we shall give concrete expressions for the boundary operator B.

According to well-established results on the spectral theory of partial differential operators (see [**1**]), there exist countably many pairs $(\lambda_n, \phi_n)_{n\in\mathbb{N}}$, with $\lambda_n \in \mathbb{R}$, $\phi_n \in H^2(U)$, such that the solutions to (2.1) can be written in the form

$$u(t,x,y) = \sum_{n=0}^{\infty} T_n(t)\phi_n(x,y),$$

where for all $n \in \mathbb{N}$ the pair (λ_n, ϕ_n) satisfies the eigenvalue problem

$$\Delta^2 \phi_n = \lambda_n^4 \phi_n \text{ in } U, \qquad B(\phi_n) = 0 \text{ on } \partial U. \tag{2.2}$$

As it is known, given $n \in \mathbb{N}$, the eigenspace defined by (2.2) is of finite dimension. Moreover, we can order the eigenvalue sequence λ_n^4 such that

$$0 \leqslant \lambda_1^4 \leqslant \lambda_2^4 \leqslant \cdots \quad \text{with } \lim_{n\to\infty} \lambda_n^4 = \infty.$$

Additionally, if

$$F(t,x,y) = \cos \lambda t \sum_{n=0}^{\infty} f_n \phi_n(x,y),$$

then T_n satisfies

$$\frac{\mathrm{d}^2 T_n}{\mathrm{d}t^2} + \left(\frac{D\lambda_n^4}{\rho h}\right) T_n(t) = f_n \cos \lambda t, \quad t \geqslant 0. \tag{2.3}$$

Roughly speaking, the vibration of the plate is a superposition of the standing waves $T_n(t)\phi_n(x,y)$, $n \in \mathbb{N}$. The eigenfunction ϕ_n is called the nth vibrational mode of the plate. Had we $\lambda^2 = D\lambda_m^4/\rho h$ for some m, then the standing wave $T_m(t)\phi_m(x,y)$ would

https://doi.org/10.1017/S0013091515000139 Published online by Cambridge University Press

become dominant and the contributions $T_n(t)\phi_n(x,y)$, $n \neq m$, could be neglected. Since the nodal lines of the mth mode of vibration $N(\phi_m)$ are at rest for all $t \geqslant 0$, the particles scattered throughout the plate tend to settle down near the nodal lines of the mth mode of vibration.

We go on reviewing some well-known examples in which the eigenpairs solving (2.2) can be given explicitly, at least up to real roots of transcendental functions.

2.1. Circular plates

In circular domains it is convenient to label the eigenpairs of (2.2) as

$$(\lambda_{nm}, \phi_{nm}), \quad n = 0, 1, \ldots, \ \ m = 1, 2, \ldots.$$

In polar coordinates (r, θ), any bounded solution of $\Delta^2 \phi_n = \lambda_n^4 \phi_n$ in a disk of radius 1 can be written as (see [**3**, Chapter 4])

$$\phi(r,\theta) = \cos(n\theta - \eta_0)(pJ_n(\lambda r) + qI_n(\lambda r)), \quad n = 0, 1, \ldots, \tag{2.4}$$

where J_n and I_n are, respectively, the Bessel function of the first kind and the modified Bessel function of the first kind. η_0 is an arbitrary constant, whereas p and q depend on the boundary conditions.

2.1.1. *All around clamped circular plates*

For circular clamped plates the boundary equation $B(\phi) = 0$ reads

$$\phi|_{r=1} = 0 = \left.\frac{\partial \phi}{\partial r}\right|_{r=1} = 0. \tag{2.5}$$

Replacing boundary conditions (2.5) in the general solution (2.4) yields

$$\begin{pmatrix} J_n(\lambda) & I_n(\lambda) \\ J_n'(\lambda) & I_n'(\lambda) \end{pmatrix} \begin{pmatrix} p \\ q \end{pmatrix} = \begin{pmatrix} 0 \\ 0 \end{pmatrix}, \tag{2.6}$$

and the characteristic equation for the clamped plate is

$$J_n(\lambda) I_n'(\lambda) - J_n'(\lambda) I_n(\lambda) = 0. \tag{2.7}$$

The value λ has to be a root of the characteristic equation (2.7) in order to guarantee the boundary condition (2.5). Now, it is known that for any $n = 0, 1, \ldots$, there are countably many solutions λ_{nm}, $m = 1, 2 \ldots$, of the characteristic equation (2.7). Table 1 shows an approximation of several of the roots λ_{nm}.

Once we determine the value λ_{nm}, the corresponding vibrational mode is easily obtained by noticing (recall (2.6)) that the coefficients p and q in (2.4) satisfy

$$pJ_n(\lambda_{nm}) + qI_n(\lambda_{nm}) = 0,$$

https://doi.org/10.1017/S0013091515000139 Published online by Cambridge University Press

Table 1. *Roots λ_{nm} of the characteristic equation for the clamped plate.*

	m			
n	1	2	3	4
0	3.1962	6.3064	9.4395	12.5771
1	4.6109	7.7992	10.9581	14.1086
2	5.9057	9.1969	12.4022	15.5795

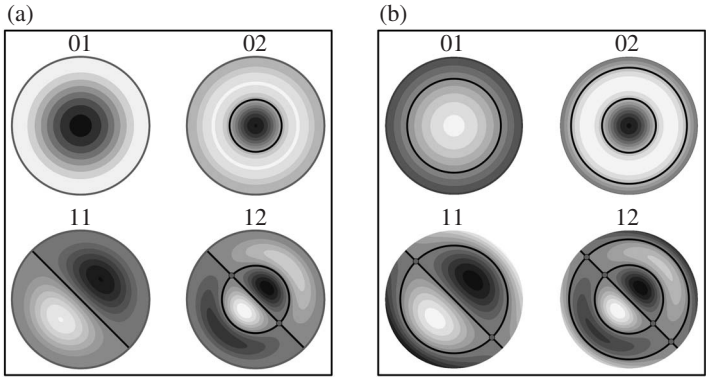

Figure 3. Nodal lines of several vibrational modes ϕ_{nm} for circular plates (the dots indicate the points in Ω at which $\nabla\phi_{nm}$ vanishes). (a) The clamped plate and (b) the free plate.

which determine p and q up to a common scalar multiple. Say that

$$\left.\begin{aligned} p &= \frac{-I_n(\lambda_{nm})}{\sqrt{J_n^2(\lambda_{nm}) + I_n^2(\lambda_{nm})}}, \\ q &= \frac{J_n(\lambda_{nm})}{\sqrt{J_n^2(\lambda_{nm}) + I_n^2(\lambda_{nm})}}, \end{aligned}\right\} \tag{2.8}$$

and the expression (up to scalar multiples) for the vibrational mode ϕ_{nm} follows:

$$\phi_{nm}(r,\theta) = \cos(n\theta - \eta_0)(pJ_n(\lambda_{nm}r) + qI_n(\lambda_{nm}r)), \tag{2.9}$$

where η_0 is arbitrary and p and q satisfy (2.8).

We now observe that for $n = 0$ the vibrational mode ϕ_{0m} spans a one-dimensional eigenspace of the eigenvalue problem (2.2) along with the clamped boundary condition. Each of these eigenspaces is made up of radially symmetric functions. Note that for $n \geqslant 1$ the eigenspace is two dimensional. Figure 3(a) illustrates $N_{\phi_{nm}}$ for $n = 0, 1$ and $m = 1, 2$. We draw attention to the fact that the circle $r = 1$ is a common nodal line of every vibrational mode for the clamped circular plate.

https://doi.org/10.1017/S0013091515000139 Published online by Cambridge University Press

Table 2. *Approximations of several roots λ_{nm} of the characteristic equation for the free plate (the value $\lambda_{00} = 0$ is omitted).*

	m			
n	1	2	3	4
0	2.971	6.1873	9.3591	12.5165
1	4.5140	7.7260	10.9008	14.0619
2	2.3637	5.9418	9.1837	12.3793

2.1.2. *All around free circular plates*

The treatment of free plates is analogous to the clamped case. The boundary condition $B(\phi) = 0$ for a circular plate with free border can be written as

$$\left.\begin{aligned}\left[\Delta\phi - \frac{1-\nu}{r}\left(\frac{\partial\phi}{\partial r} + \frac{1}{r}\frac{\partial^2\phi}{\partial\theta^2}\right)\right]\Big|_{r=1} &= 0,\\ \left[\frac{\partial}{\partial r}(\Delta\phi) + \frac{1-\nu}{r}\frac{\partial}{\partial r}\left(\frac{1}{r}\frac{\partial^2\phi}{\partial\theta^2}\right)\right]\Big|_{r=1} &= 0.\end{aligned}\right\} \tag{2.10}$$

Writing the Laplacian in polar coordinates and replacing the set of boundary conditions on (2.4), we obtain the characteristic equation for the free circular plate. The resulting expression is a bit more elaborate than (2.7). We omit the details and refer the reader to [**3**, Chapter 4] for a more complete discussion. The main point is that, given $n = 0, 1, \ldots,$ we can compute the sequence λ_{nm} of zeros of the characteristic equation of the free circular plate and obtain, analogous to the procedure for the clamped circular plate, the expressions of the corresponding vibrational modes.

Table 2 shows some of the roots of the characteristic equation for the free circular plate. Here we omit the first value $\lambda_{00} = 0$ since the term $\cos\lambda_{00}t$ has no clear meaning as an external harmonic force in (2.3). The nodal lines of circular clamped and free plates look similar (see Figure 3), but $r = 1$ is never a nodal line of the vibrational modes ϕ_{nm} of the free plate.

2.2. General domains

Solutions to (2.2) are known to be smooth in bounded domains U. Moreover, if $\phi_n^1, \ldots, \phi_n^k$ span the eigenspace corresponding to the nth eigenvalue λ_n^4, then

$$\phi_n^i \in C^\infty(U) \cap C(\bar{U}), \quad i = 1, \ldots, k.$$

Regularity at the boundary ∂U is a matter that depends on the smoothness of the boundary itself. In domains with corners, it can be difficult to guarantee the existence of, say, the second derivatives of the vibrational modes at the corner points. We refer the reader to [**8**, Chapter 3] for more details on the existence and regularity of solutions to the eigenvalue problem we consider.

https://doi.org/10.1017/S0013091515000139 Published online by Cambridge University Press

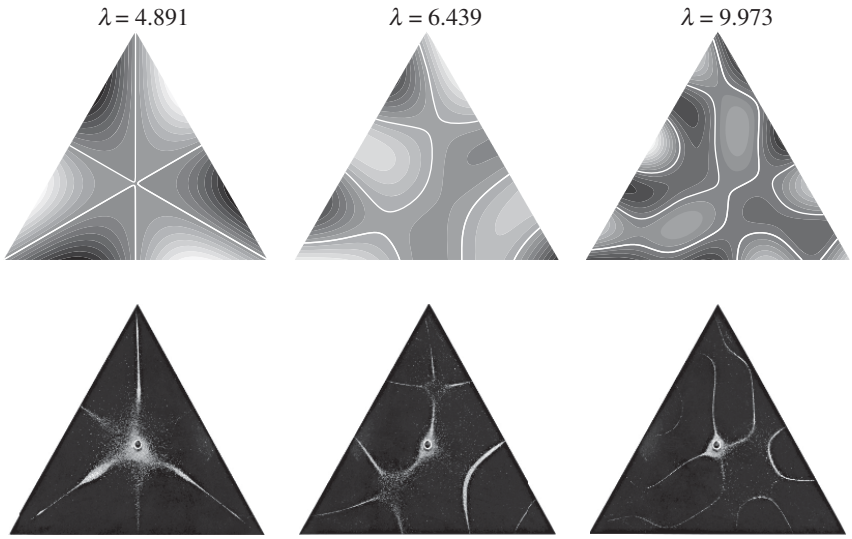

Figure 4. Nodal lines (white) of an equilateral triangular plate under free boundary condition (above). The corresponding Chladni figures were obtained through home-made experiments carried out by the authors (below).

Table 3. *Values λ_n for an equilateral triangular plate with all around free border (the value $\lambda_0 = 0$ is omitted).*

n	1	2	3	4	5	6	7	8	9
λ_n	2.93	3.06	4.63	4.89	5.43	6.37	6.43	7.33	8.14

In general domains it is necessary to draw upon numerical approximations to compute the eigenpairs (ϕ_n, λ_n^4) (see, for example, [**7**]). We used FreeFem++ [**10**] to compute eigenpairs under free as well as clamped boundary conditions in several domains; for example, in an equilateral triangle. In Table 3 we list the first nine values of λ_n and in Figure 4 we illustrate the level sets of some of the vibrational modes as well as their corresponding Chladni figures, obtained through home-made experiments by the authors. We refer the reader to the beautiful illustrations crafted by Chladni himself in his book *Die Akustik* [**4**]. Chladni drew the figures for the equilateral triangle in pictures 219–243 (see [**4**, p. 281].

3. A stochastic model

It is tempting to think of Chladni's experiment as the result of the kicks that the bending plate impinge on the particles when the external force resonates with one of the natural frequencies of the plate. When several modes of vibration contribute to the bending, they tend to cancel each other and as a result the particle translation is barely noticeable. The energy transmitted to a particle can be assumed to be proportional to the bending

https://doi.org/10.1017/S0013091515000139 Published online by Cambridge University Press

amplitude. On the other hand, the jumps of a particle are random due to its shape, the roughness of the plate and the phase time between the frequency of the plate and the frequency by which particles bump the plate. Now, since the plate will be moving upwards when it hits a particle one could expect the particle's movement to be biased toward the opposite direction to the gradient of the resonating mode ϕ. In this sense Assumption 1.1 (2) is more general since it asks only that the outward normal vector to a nodal line and the drift of a particle form an angle $-\pi/2 < \theta < \pi/2$ at nodal points where $\nabla\phi \neq 0$.

We may think of the particle's motion as the limiting case of a discrete stochastic process obeying the following axioms.

(1) The particles move independently of each other.

(2) Any particle's motion is described by a stochastic process $(X_n)_{n=0}^{\infty}$, where X_n represents its position after the nth jump. We agree to the convention that $X_n = q$ for all $n \geqslant n_0$ whenever $X_{n_0-1} \in U$ and $X_{n_0} = q$ with $q \notin U$.

(3) The jumps $X_{n+1} - X_n$ are independent random variables having a two-dimensional vector mean μ_n such that

$$X_{n+1} - X_n = \mu_n + \sigma_n \xi_n, \tag{3.1}$$

where ξ_n are independent identically distributed random variables having mean zero, covariance matrix I (the 2×2 identity matrix), possess a finite $(2+\delta)$th absolute moment for some $\delta > 0$ and have a bounded or square-integrable density. Regarding μ_n and σ_n, we assume

$$\mu_n = \delta t \mu_\phi(X_n)\nabla\phi(X_n), \qquad \sigma_n = \sqrt{\delta t}\sigma_\phi(X_n),$$

where μ_ϕ and σ_ϕ fulfil Assumption 1.1 and $\delta t > 0$ is constant.

We see that (3.1) defines a generalized Euler–Maruyama approximation with step size δt for the solution of the stochastic differential equation

$$\mathrm{d}X_t = \mu_\phi(X_t)\nabla\phi(X_t)\,\mathrm{d}t + \sigma_\phi(X_t)\,\mathrm{d}W_t, \quad X_0 = x, \tag{3.2}$$

where W_t is a standard two-dimensional Brownian motion.

As we highlighted in § 2.2, the modes of vibration ϕ are smooth in U and continuous in $\bar{U}$. We assume there is a C^2 compact support extension of the vibrational mode ϕ such that (3.2) fulfils the standard existence and uniqueness theorem of SDEs (see, for example, [**13**, Chapter 6]) and that any solution is defined for all $t \geqslant 0$. Solutions of (3.2) starting at $x \in U$ at $t = 0$ will be denoted by X_t^x. If the context is clear, the superscript x will be omitted.

On the other hand, it is known that the mode of vibration ϕ as well as its gradient $\nabla\phi$ are bounded in U for clamped and free plates (see, for example, [**8**]). As a consequence, we may assume that the compact support extension of the vibrational mode is such that

$$\|\mu_\phi(x)\nabla\phi(x)\| + \|\sigma_\phi(x)\| \leqslant L, \quad x \in \mathbb{R}^2, \tag{3.3}$$

https://doi.org/10.1017/S0013091515000139 Published online by Cambridge University Press

for some positive constant L. Taking into account axioms (1), (2) and (3) and inequality (3.3), we can apply a result of Kanagawa [**12**] to guarantee that the polygonal continuous interpolation defined by (3.1), with starting value x, weakly converges, in the sense of the L^p-Wasserstein metric, $p \geqslant 1$, to the unique solution X_t^x of (3.2). We refer the reader to [**15**, § 10.3] for a deeper discussion of the Wasserstein metric and the approximation of SDEs.

Furthermore, we note that Assumption 1.1 (1) guarantees that any point of the nodal lines of ϕ is an equilibrium of (3.2). The main result of this paper pertains to the stochastic stability of the equilibria of (3.2), which coincide with the Chladni figure of the corresponding mode.

It is known that (3.2) defines a probability space on the sample set Ω of trajectories of (3.2). We denote by P the probability function on this space. For the reader's convenience we recall the definition of a stochastically stable equilibrium, and refer the reader to [**13**] for a more detailed discussion.

Definition 3.1. We say that q_0 is a stochastically stable equilibrium of (3.2) if, for every $\varepsilon > 0$,

$$\lim_{q \to q_0} P\Big[\sup_{0 \leqslant t < \infty} |X_t^q - q_0| \geqslant \varepsilon \Big] = 0.$$

In the case of clamped plates, the boundary ∂U is itself a nodal line of ϕ. Thus, any solution to (3.2) starting in U will remain in U with probability 1. For free plates the matter is different: a solution to (3.2), X_t, starting at U may leave U in a finite time with a non-vanishing probability.

The stability result in our investigations will depend heavily on the application of Itô's formula. It will be convenient to define the following elliptic operator L, closely related to the infinitesimal generator of the stochastic process given by SDE (3.2):

$$L = \sum_{i,j=1}^{2} a_{ij} \frac{\partial^2}{\partial x_i \partial x_j} \quad \text{with } (a_{ij}) = A.$$

By Assumption 1.1 (3), L is uniformly elliptic on a neighbourhood of $\bar{U}$, and notice that for SDE (1.1), L coincides with the Laplace operator Δ. For a given subdomain $D \subset U$ and a given non-constant function $g \in C^{2,\gamma}(\bar{D})$, with $\gamma > 0$ (where the notation follows [**9**]), we shall consider the boundary-value problem

$$Lv = 0 \text{ in } D, \qquad v = g \text{ on } \partial D. \tag{3.4}$$

If ∂D is made up of regular boundary points (we refer the reader to the definition of regular boundary points of elliptic operators in [**9**, Chapter 8]), it is known that (3.4) possesses a unique solution $v \in C^2(D) \cap C(\bar{D})$. Furthermore, $u \in C^2(D \cup \Gamma)$ provided that Γ is a C^2 piece of ∂D. Also, by the maximum principle, we have that $0 < v < 1$ in D whenever $0 \leqslant g \leqslant 1$ on ∂D.

A point $x_0 \in N_\phi$ is called a critical point if $\nabla \phi(x_0)$ vanishes or does not exist.

Theorem 3.2. *If Assumption 1.1 is fulfilled, then any non-critical point of N_ϕ is a stochastically stable equilibrium of SDE (3.2).*

https://doi.org/10.1017/S0013091515000139 Published online by Cambridge University Press

Proof. Let $x_0 \in N_\phi \cap U$ be a non-critical point. Since N_ϕ is locally a regular curve at x_0, there exists $\varepsilon > 0$ such that N_ϕ splits $B_\varepsilon(x_0)$ into two sub-domains of U in which ϕ has definite sign. For any of these domains $D \subset U$, let us define a continuous function g on ∂D such that $g(x_0) = 1$, $g(x) = 0$ when $|x - x_0| = \varepsilon$ and $0 \leqslant g \leqslant 1$. We shall assume that g admits a $C^{2,\gamma}(\bar{D})$ extension.

Now, consider the unique solution v to boundary-value problem (3.4). By Hopf's boundary-point lemma, $\nabla v(x_0)$ points in the outward direction of D. Moreover, for some non-vanishing scalar λ we have $\nabla v(x_0) = \lambda \nabla \phi(x_0)$ with $\operatorname{sign}(\lambda) = -\operatorname{sign}(\phi)$. By Assumption 1.1 (2), there exists a neighbourhood V of x_0 such that

$$\operatorname{sign}(\nu_\phi(x)\nabla\phi(x) \cdot \nabla v(x)) = \operatorname{sign}(\lambda) = -\operatorname{sign}(\phi(x)) = \operatorname{sign}(f(\phi(x)))$$

for $x \in V \cap D$. Thus, $\mu_\phi(x)\nabla\phi(x) \cdot \nabla v(x) \geqslant 0$ for $x \in V \cap D$. Furthermore, one may choose V such that $\partial(V \cap D) \subset N_\phi \cup \{x \in D \colon v(x) = \delta\}$ for some $0 < \delta < 1$.

By Itô's formula, we have

$$E[v(X_t)] = v(x) + E\bigg[\int_0^t \mu_\phi(X_s)\nabla\phi(X_s) \cdot \nabla v(X_s) + \tfrac{1}{2}(\sigma_{11}^2(X_s) + \sigma_{22}^2(X_s))Lv(X_s)\,\mathrm{d}s\bigg],$$

where $\sigma(x) \equiv \sigma_\phi(x)$. Denote by τ_δ the hitting time of X_t with $\partial(D \cap V)$ and let $T > 0$. We have

$$E[v(X_{T\wedge\tau_\delta})] = v(x) + E\bigg[\int_0^{T\wedge\tau_\delta} \mu_\phi(X_s)\nabla\phi(X_s) \cdot \nabla v(X_s)\,\mathrm{d}s\bigg] \geqslant v(x).$$

On the other hand, since N_ϕ is not attainable (see [**6**, Chapter 13]), we have

$$E[v(X_{T\wedge\tau_\delta})] = \int_{\tau_\delta > T} v(X_T)\,\mathrm{d}P + \delta P(\tau_\delta \leqslant T) \leqslant P(\tau_\delta > T) + \delta P(\tau_\delta \leqslant T),$$

and so

$$P(\tau_\delta > T) + \delta P(\tau_\delta \leqslant T) \geqslant v(x).$$

This implies that

$$(1 - \delta)P(\tau_\delta > T) = P(\tau_\delta > T) + \delta(P(\tau_\delta \leqslant T) - 1) \geqslant v(x) - \delta.$$

Letting $T \to \infty$, we finally obtain

$$P(\tau_\delta = \infty) \geqslant \frac{v(x) - \delta}{1 - \delta},$$

and therefore $P(\tau_\delta = \infty) \to 1$ as $x \to x_0$, $x \in D$, so x_0 is a stochastically stable equilibrium of (3.2).

If $x_0 \in \partial U$ is a non-critical point, we can repeat the above argument to obtain the stability result. However, outside the domain U, the model does not represent the motion of the particles in Chladni's experiment. □

https://doi.org/10.1017/S0013091515000139 Published online by Cambridge University Press

The question remains as to whether critical points of N_ϕ are stochastically stable in the general model (3.2). Sadly, the technique of the above proof fails to determine the non-negativity of the expression $\nu_\phi(x)\nabla\phi(x)\cdot\nabla v(x)$ for $x\in V\cap D$, rendering the argument useless when $\nabla\phi(x_0)=0$.

We know for sure that, for any vibrational mode ϕ of the circular free plate, there are only finitely many critical points in N_ϕ, which are precisely the crossings of the radial lines and the circular lines of N_ϕ as shown in Figure 3(b). However, for the clamped plate, in addition to finitely many isolated singular points, the border of the circle is a line of critical points of N_ϕ. Regarding convex domains with free boundary condition, numerical experimentation suggests that N_ϕ has a similar structure to the nodal lines of the free circular plate (see, for example, Figure 4 or [**7**, Figure 4.1]). We know in general that the vibrational modes are real analytic in U, which implies that $U\cap N_\phi$ is locally the union of finitely many isolated points and arcs (homomorphic images of $[0,1]$), where arcs are analytic, except possibly at isolated points.

Definition 3.3. We say that $x_0\in N_\phi$ is a nodal regular point if there exists $\varepsilon>0$ such that N_ϕ splits $B_\varepsilon(x_0)$ into a finite number of sub-domains D_i such that ∂D_i is made up of regular boundary points for the operator L.

The condition to be a nodal regular point is relatively weak. It is satisfied by non-critical points, cusp points, crossing points of several nodal arcs, and the end points of loose arcs in N_ϕ. We succeed in proving the stochastic stability of any nodal regular point of N_ϕ, though only in a particular case of (3.2).

Theorem 3.4. *If Assumption 1.1 is fulfilled, then any nodal regular point of N_ϕ is a stochastically stable equilibrium of*

$$\mathrm{d}X_t=\sigma_\phi(X_t)\,\mathrm{d}W_t.$$

Proof. We solve problem (3.4) in each of the sub-domains D_i in which N_ϕ splits $B_\varepsilon(x_0)$ with a continuous boundary function g_i defined on ∂D_i such that $g_i(x_0)=1$, $g_i(x)=0$ when $|x-x_0|=\varepsilon$, and $0\leqslant g_i\leqslant 1$. The rest is step by step the proof of Theorem 3.2. □

Isolated points of N_ϕ are not nodal regular points and they need not be stochastically stable equilibria. The following calculation shows this for equilibrium $(0,0)$ of the SDE

$$\mathrm{d}X_t=|X_t|\,\mathrm{d}W_t.$$

The above equation can be written in polar coordinates $R_t=|X_t|$ and $\theta_t=\arg(X_t)$ to obtain the explicit solution

$$R_t=R_0\mathrm{e}^{W_r(t)},\qquad \theta_t=\theta_0+W_\theta(t),$$

where $W_r(t)$ and $W_\theta(t)$ are standard one-dimensional Brownian processes while R_0 and θ_0 are the starting values of R_t and θ_t respectively. Clearly, the equilibrium $(0,0)$ is unstable.

https://doi.org/10.1017/S0013091515000139 Published online by Cambridge University Press

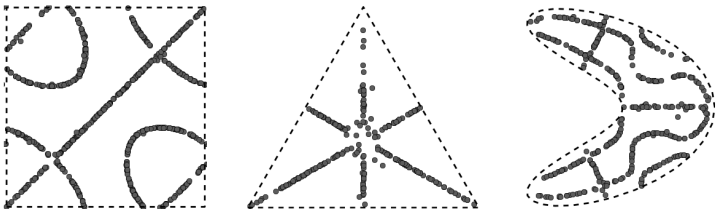

Figure 5. Final positions of some trajectories of (1.1) ($\alpha = 0$, $\beta = 1$) starting at an initial grid of random points uniformly distributed.

4. Numerical experiments

Computing plate vibrational modes is a well-established trade associated with the development of free and commercial software. In this investigation we made use of FreeFem++, Version 3.23 [**10**] and a good deal of self-made Python code, using standard Python libraries such as MatPlotLib, SciPy and NumPy [**14**], to compute the vibrational modes ϕ in several regions U under free and clamped boundary conditions.

The stochastic simulations to obtain Figures 1 and 5 implement the Euler–Maruyama method [**11**] with a step size parameter δt and a final T simulating $T = \infty$ tailored to the vibrational mode ϕ. Figure 5 is a collage of the outcomes of numerical simulations in several regions U: a square, an equilateral triangle and a boomerang-like region, all of them with free border. We start from an initial grid of random points uniformly distributed in U, then we numerically approximate the solution to (1.1) (with $\alpha = 0$) and show the final position of the particles.

Acknowledgements. The authors thank Professor M. Marmolejo and Professor A. Gómez for helpful discussions during the preparation of the paper and La Universidad del Valle for providing the academic environment to carry out this investigation. They are also in debt to the anonymous referee for carefully reading the manuscript and for pointing out valuable generalizations and improvements of the SDE model.

References

1. S. Agmon, On the eigenfunctions and on the eigenvalues of general elliptic boundary value problems, *Commun. Pure Appl. Math.* **15** (1962), 119–147.
2. G. Bradski, The OpenCV Library, Dr Dobb's J. Software Tools (2000).
3. S. Chakraverty, *Vibration of plates* (CRC Press, 2009).
4. E. Chladni, *Die akustik* (Breitkopf and Härtel, Leipzig, 1802) (available at http://vlp.mpiwg-berlin.mpg.de/references?id=lit29494).
5. M. Faraday, On a peculiar class of acoustical figures; and on certain forms assumed by groups of particles upon vibrating elastic surfaces, *Phil. Trans. R. Soc. Lond.* **121** (1831), 299–340.
6. A. Friedman, *Stochastic differential equations and applications* (Dover, New York, 1975).
7. M. Gander and F. Kwok, Chladni figures and the Tacoma Bridge: motivating PDE eigenvalue problems via vibrating plates, *SIAM Rev.* **54**(3) (2012), 573–596.
8. F. Gazzola, H. Grunau and G. Sweers, *Polyharmonic boundary value problems*, Lecture Notes in Mathematics, Volume 1991 (Springer, 2010).

9. D. Gilbarg and N. Trudinger, *Elliptic partial differential equation of second order* (Springer, 1991).
10. F. Hecht, FreeFem++, Version 3.23 (6 July 2013; available at www.freefem.org/ff++).
11. D. Higham, An algorithmic introduction to numerical simulation of stochastic differential equations, *SIAM Rev.* **43**(3) (2001), 525–546.
12. S. Kanagawa, The rate of convergence for approximate solutions of stochastic differential equations, *Tokyo J. Math.* **12**(1) (1989), 33–48.
13. A. Ludwig, *Stochastic differential equations* (Wiley, 1974).
14. T. Oliphant, Python for scientific computing, *Comput. Sci. Engng* **9**(3) (2007), 10–20.
15. S. Rachev and L. Rüschendorff, *Mass transportation problems, part II: applications*, Probability and Its Applications (Springer, 1998).